CARBON 49 (2011) 2555–2560

available at www.sciencedirect.com

ScienceDirect

journal homepage: www.elsevier.com/locate/carbon

Enrichment of metallic carbon nanotubes by electric field-assisted chemical vapor deposition

Banghua Peng [a,b], *Shan Jiang* [a], *Yongyi Zhang* [a], *Jin Zhang* [a,*]

[a] *Center for Nanochemistry, Beijing National Laboratory for Molecular Sciences (BNLMS), Key Laboratory for the Physics and Chemistry of Nanodevices, State Key Laboratory for Structural Chemistry of Unstable and Stable Species, College of Chemistry and Molecular Engineering, Peking University, Beijing 100871, China*

[b] *School of Chemistry and Chemical Engineering, Shihezi University, Xinjiang 832000, China*

ARTICLE INFO

Article history:
Received 1 December 2010
Accepted 15 February 2011
Available online 17 February 2011

ABSTRACT

We report herein a rational approach to increase the proportion of metallic carbon nanotubes (CNTs) in horizontally aligned ultralong CNT arrays by electric field-assisted chemical vapor deposition. In a gas flow-directed growth mode, the buoyancy caused by temperature differences near the substrate can lift catalyst particles or CNTs from the substrate into the laminar flow so that ultralong CNT arrays with mixed metallic (*m*-) and semiconducting (*s*-) CNTs can be obtained. It was verified that the percentage of *m*-CNTs was about 47% for pristine CNTs. When an electric field was introduced during CNT growth, the grown CNTs were polarized and the generated electric field force assisted them into the laminar flow. The greater polarizability of *m*-CNTs compared to *s*-CNTs resulted in more *m*-CNTs lifted and an increased *m*- to *s*-CNT ratio in the array. Measurements of CNT electrical properties showed that the percentage of *m*-CNTs could reach 80% when the electric field intensity was set at 200 V/cm.

1. Introduction

Carbon nanotubes (CNTs) have been regarded as one of the best candidates for nanoelectronic devices due to their unique electronic structure and superior electrical properties [1,2]. Semiconducting (*s*-) CNTs can be used to fabricate field-effect transistors and used in logic circuits. Metallic (*m*-) CNTs are ideal materials for use in single electron transistors and in interconnections due to their excellent current carrying capacity, exceeding 10^9 A/cm^2 [3–6]. Current CNT fabrication techniques can only produce a mixture of *m*- and *s*-CNTs, which remains an obstacle to their application. Therefore, it will be critical to develop efficient techniques for separating *m*- or *s*-CNTs from pristine mixtures for their application in devices. Many groups have been devoted to approaches such as electrophoresis [7], density gradient induced centrifugation [8] and gas-phase plasma etching [9]. All of these can effectively separate *s*- or *m*-CNTs with very high purity. However, the CNTs are inevitably chemically decorated, damaged or contaminated during the separation process.

In order to solve this problem, protocols for the selective growth of certain types of CNTs have been developed. This earlier work reported to directly grow *s*-CNTs using plasma enhanced chemical vapor deposition (CVD) [10]. By using an ethanol/methanol mixture as a carbon source and Cu nanoparticles as catalysts, *s*-CNT arrays can be directly grown on ST-cut single-crystal quartz substrates [11]. Recently, our group also developed an approach to grow *s*-CNTs by introducing UV irradiation during the CVD process [12]. Although some progress has been made in controlling the growth of CNTs, most work has been focused on the separation of *s*-

* *Corresponding author:*
E-mail address: jinzhang@pku.edu.cn (J. Zhang).
0008-6223/$ - see front matter
doi:10.1016/j.carbon.2011.02.045

CNTs and no approaches have offered detailed explanations of the mechanisms causing separation. Little research has been carried out on the direct growth of *m*-CNTs except the work of Harutyunyan et al. [13]. The development of reliable techniques for preferentially synthesizing *m*-CNTs during growth would be a significant advancement towards the widespread applicability of CNTs in electronic devices. Therefore, selective growth of *m*-CNTs remains a significant challenge for researchers.

Electric fields (EF) have been used to direct CNT growth [14–18], but there have been no related reports about selective effects on CNTs' grown using EF-assisted CVD. *m*- and *s*-CNTs differ greatly in their permittivity and conductivity, and would thus be impacted differently by the EF. Based on this viewpoint, we report herein a rational approach to increase the percentage of *m*-CNTs in horizontally aligned CNTs array by EF-assisted CVD. Ultralong CNTs arrays were developed using EF-assisted CVD, and it was found that the ratio of *m*-CNTs to *s*-CNTs in the as grown CNT arrays was enhanced by the EF effect. Electrical property measurements indicated that CNT arrays containing about 80% *m*-CNTs can be obtained using an EF intensity of 200 V/cm.

2. Sample preparation

Ultralong CNTs were grown in a low pressure CVD system (Tystar Corporation, USA). 0.01 M $FeCl_3$ in ethanol was used as a catalyst precursor and was stamped using polydimethyl siloxane (PDMS) in a striped pattern on 800 nm thermally oxidized p-type silicon substrates. The furnace was heated up to 950 °C in 20 min at 650 Torr under a flow of 800 sccm (standard cubic centimeter per minute) Ar and 400 sccm H_2. Nanotubes were then grown using ethanol (kept at 45 °C) as the carbon source, which was bubbled with 60 sccm Ar for 30 min. Meanwhile, a direct-current (DC) EF was introduced. Finally, the carbon feed was stopped and the EF was shut down.

Ultralong CNTs were grown on SiO_2/Si substrates. The substrates were put into the CVD system horizontally under the electrodes with the catalyst lines facing the gas flow (Fig. 1a). Electrodes were fixed horizontally with metal fastener on a quartz board and metal wire, connected to the electrodes, was stretched out of the CVD along two metal poles separately and joined to a DC power source to transfer voltage (electrode configuration and installation are shown in Figure S1). It was clear that ultralong CNTs arrays can be grown without EF (Fig. 1b), but well-aligned ultralong CNTs arrays did not appear under EF-assisted CVD. Fig. 1c–f illustrate the EF effect on the CNTs' growth. After increasing EF intensity, almost no CNTs grew and most CNTs stopped growing at catalyst areas, demonstrating the violent disturbing effect of the EF on CNTs' growth. Higher EF intensities above 500 V/cm prevent any ultralong CNTs from growing from the catalyst areas (Figure S2). Most of our experiments were carried out below an EF intensity of about 500 V/cm to obtain ultralong CNTs to investigate the EF effect on *s*- and *m*-CNTs.

3. Characterization of carbon nanotubes

To test the EF effect on ultralong CNTs' growth, we characterized structural and electrical properties of CNTs grown under EF-assisted CVD. Forty CNTs grown under an EF intensity of 200 V/cm were imaged by AFM (Fig. 2a), and the average diameter of the CNTs was found to be about 2.6 nm. To confirm the actual structure of the sample, we transferred the CNTs [19] to a TEM grid. TEM imaging demonstrated that most of the CNTs were double-walled carbon nanotubes (DWCNTs) and single-walled carbon nanotubes (SWCNTs) (Fig. 2b and c). Because not all the CNTs are SWCNTs, the structure and the attribute of our CNTs can not be determined clearly by single wavelength Raman spectroscopy. On the contrary, the Raman characterization sometimes gave the wrong estimation about the EF's effect on CNTs' separation for DWCNTs' coexisting. In order to analyze the separation effects of EF-assisted CVD, electrical properties of CNTs grown under various EF intensities far from the catalysts were measured. The test electrodes were fabricated using electron beam lithography and subsequent thermal evaporation of Cr (5 nm) and Au (45 nm). Detailed procedures are described in the SI, Part C. Fig. 2d shows a representative SEM image of electrodes on a sample – the CNTs are indiscernible at this scale, but are present between the electrodes.

During measurements of CNT electrical properties, the ON/OFF ratio (ration of maximum current and minimum current in electrical measurement currents) was used as the criterion for distinguishing *m*- or *s*-CNT. If the gate voltage (V_g) could modulate the current between the source and drain electrodes (I_{ds}) and the ON/OFF ratio was above 100 for one

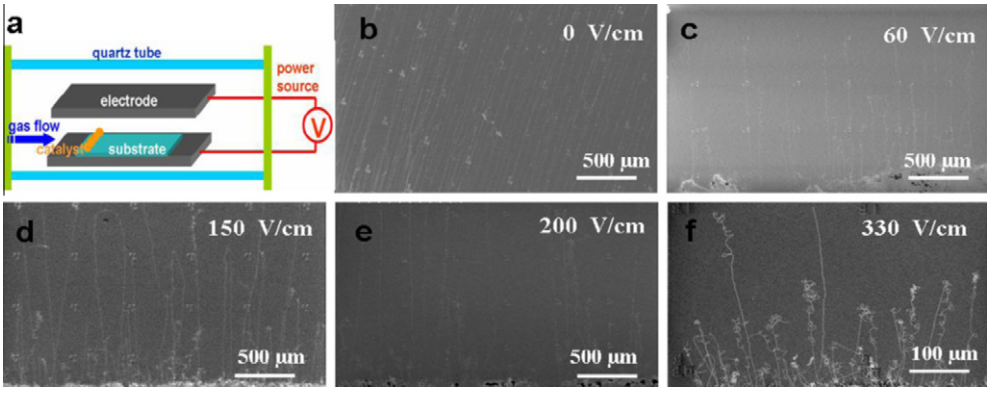

Fig. 1 – SEM images of the effect of an electric field on the growth of ultralong CNTs.

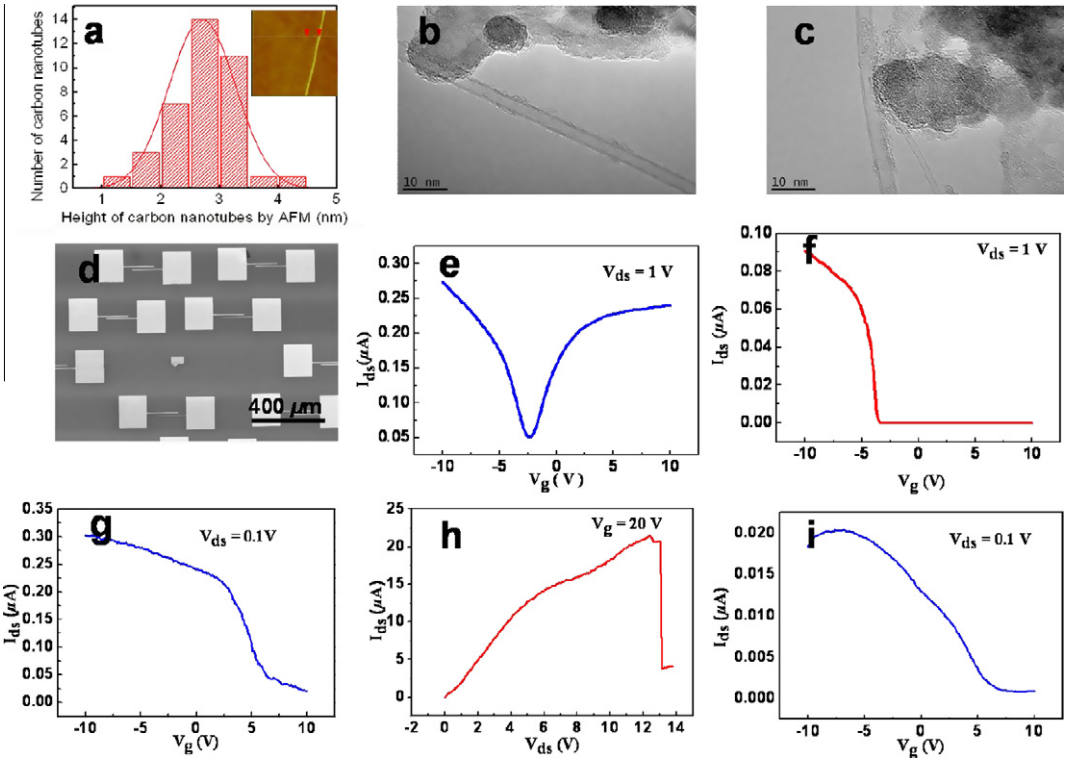

Fig. 2 – Characterization of CNTs by AFM, TEM and related measurements of electrical properties.

CNT, the CNT was classified as semiconducting. Otherwise, it was considered an *m*-CNT. Fig. 2e and f presents typical I_{ds}–V_g curves for *m*- and *s*-SWCNTs, respectively. For SWCNTs, it is easy to distinguish their metallic or semiconducting attribute for their simple structure and obvious difference in electrical property measurements. While for DWCNTs, it is hard to do. DWCNTs have four distinct shell-shell combinations [20]: metallic outer layer-semiconducting inner layer (*m*–*s*), *m*–*m*, *s*–*m*, and *s*–*s*. Among the four types of DWCNTs, the *s*–*m* DWCNTs were difficult to distinguish because the I_{ds}–V_g curves present small ON/OFF ratios of about 10 (Fig. 2g) [20]. The curve differed from *m*-CNT curves because current would change with the gate voltage, but the modulation was less pronounced than that seen with *s*-CNTs [21]. In order to confirm the structure, the electrical breakdown technique was applied to remove the inner *m*-CNT during measurement process [22–23] (Fig. 2h). Electrical measurements after the breakdown showed a large ON/OFF ratio like in Fig. 2i, we could then confirm that the DWCNT configuration was *s*–*m*.

We classified the *m*–*s*, *m*–*m*, and *s*–*m* DWCNTs as metallic tubes and the *s*–*s* DWCNTs as semiconducting tubes based on the work by Kozinsky B. [24]. (See next section: Discussion about the EF effect on CNTs. Kozinsky B.'s work showed that the axial polarizability of multi-walled CNTs was the sum of that of every shell. The EF can affect *m*–*m*, *m*–*s*, and *s*–*m* DWCNTs due to their greater axial polarizability, but not does on the *s*–*s* DWCNTs). Assuming that the two shells of the DWCNTs are totally independent, metallic DWCNTs should make up approximately 5/9 of all the CNTs [23]. We tested the CNT sample grown without an added EF and found that it consisted of 46.7% *m*-CNTs, which is accordance with the theoretic record. Despite these results, we still obtained ultralong CNT arrays containing about 80% *m*-CNTs far from the catalyst regions under EF-assisted CVD.

Table 1 gives the statistical results regarding *m*- and *s*-CNTs on samples grown under different EF intensities. As the intensity of the EF was increased, CNT arrays with high percentages of *m*-CNTs grew from the catalysts. At EF intensities of around 200 V/cm, the proportion of *m*-CNTs in our ultralong CNT arrays could reach about 80%.

Table 1 – Statistical results of I_{ds}–V_g measurements of *m*-CNTs and *s*-CNTs under different direct-current (DC) EF intensities.

Sample	EF intensity	Number of *m*-CNTs	Number of *s*-CNTs	*m*-CNTs %
1	0 V/cm	35	40	46.7
2	DC, 80 V/cm	12	9	57.1
3	DC, 150 V/cm	26	14	65.0
4	DC, 200 V/cm	38	8	82.3

4. Discussion

For gas flow-directed ultralong CNTs' growth, the growth process can be divided into two stages. During the first stage of growth, buoyancy lifts CNTs or catalyst particles into the laminar gas flow so that the growing CNTs will be aligned by the

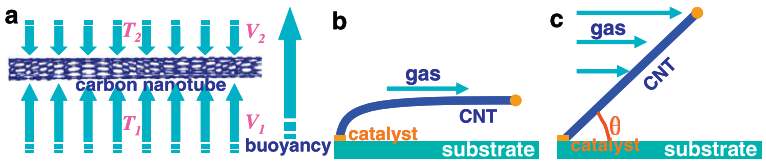

Fig. 3 – Force analysis for CNT caused by molecules colliding and gas flow during CVD growth.

gas flow during the second stage [25–29]. Therefore, the buoyancy and gas flow orientation forces were the two main factors in aligning CNTs on surface. When an EF was loaded during CNT growth, the EF would also affect CNTs' growth.

Buoyancy is the vertical motion of gas flow caused by gas density differences [29,30]. Pressure and temperature gradients lead to gas flow density gradients and impel this motion, which makes the gas flow transfer vertically, driving the CNTs to float. The buoyancy forces on a CNT can be considered as the momentum changes of molecule bumping against the CNT in a determinate period. Given a CNT with radius $R = 1$ nm and length $L = 500$ μm floating horizontally in the gas flow (Fig. 3a), and a pressure difference P_1–P_2 between the top and bottom of the CNT of about 0.001 Pa, we arrive at a calculated buoyancy of about 10^{-15} N. (See the buoyancy calculation in the part D, SI.) Alternatively, we can make calculations based on the temperature difference T_1–T_2 in formula (6) in SI to calculate the buoyancy. The larger the pressure or temperature difference, the greater the buoyancy is. From our above analysis, buoyancy is so weak as to have no apparent effect on CNTs' growth. Actually, in our CVD system, the flowing gas was heated to the reaction temperature before arriving at the substrate [30] and there would have been little pressure or temperature difference that could cause gas flow circulation. Therefore, we conclude that buoyant forces are insignificance and their effects on CNTs' growth can be ignored.

For the gas flow orientation force, we consulted fluid mechanics theory [31]. If CNTs are parallel to the substrate, the gas flow shear force is the main force operating on the CNTs (Fig. 3b). The detailed computation process is given in the part E in SI. For CNTs of $L = 500$ μm, the gas flow shear force is about 3.4×10^{-13} N.

If CNTs deviated from the gas flow direction with angle θ to the substrate (illustrated in Fig. 3c), the gas flow orientation force is primarily rooted in the gas flow drag force. The gas flow shear force and drag force are both part of the gas flow orientation force, but the gas flow drag force is much larger than the shear force and holds a large projected area vertical to the gas flow direction. The drag coefficient, depending on the aspect ratio of the CNT, is much larger than the shear force coefficient [31]. So for the acclivitous CNTs, the gas flow drag force is much larger than gas flow shear force and is the primary factor in ultralong CNT orientation. Because the drag force coefficient is difficult to compute, we are only able to conclude that the gas flow orientation force is larger than a pico-Newton.

When an EF was applied during CNTs' growth, the CNTs would have been polarized [32] and thus an EF force was generated [14]. This polarization was anisotropic for CNTs [32]. For ultralong CNTs, axis polarizability usually dominates while that along the radius is often neglected. During the CNTs' growth, the EF was perpendicular to the CNTs; thus, the resulting vertical EF force would cause CNTs to be lifted up in the horizontal direction [14]. This would be helpful for ultralong CNTs' growth, making them grow more readily from catalyst particles. In general, *m*-CNTs are more polarizable than *s*-CNTs along their axes [32] according to the polarizability expression of α_{zz} for *m*- and *s*-CNTs [14]:

$$\alpha_{zz}^{m} = \frac{L^2}{24[\ln(L/R) - 1]}\left[1 + \frac{4/3 - \ln 2}{\ln(L/R) - 1}\right] \quad (1)$$

$$\alpha_{ZZ}^{s} = 17.8 \times \frac{R}{E_g^2} \quad (2)$$

Using these equations we can calculate CNT's polarizability. Supposing CNT's length $L = 500$ μm and radius $R = 1$ nm, the computed polarizability differs greatly based on electronic type, at about 9.0×10^{10} Å^2 for *m*-CNTs and 1.1×10^3 Å^2 for *s*-CNTs [32]. The EF thus produces an EF force, which would make the CNTs align with the EF direction. The EF force for CNTs is expressed by [15]:

$$F_E = 1/2\alpha_{ZZ}E^2 \cdot \sin 2\theta \cdot 4\pi\varepsilon_0 = 2\pi\varepsilon_0 \cdot \alpha_{zz}E^2 \cdot \sin 2\theta \quad (3)$$

Here ε_0 is the absolute permittivity of air, E represents the EF intensity and θ is the angle between EF line and the CNT. Using the given parameters, we can calculate an EF force of 2.0×10^{-11} N on *m*-CNTs and 2.3×10^{-19} N on *s*-CNTs. The longer the CNTs are, the greater the difference about the EF force between the *m*-CNTs and *s*-CNTs is. Based on this data, we think the EF force only has a significant effect on *m*-CNTs because the EF force is several orders of magnitude greater for *m*-CNTs than for *s*-CNTs. Especially, after calculating rotation energies [14] (see calculations for EF rotation energy about *m*- and *s*-CNTs in Part F, SI), we find that the EF rotation energy for *m*-CNTs is also much larger than that for *s*-CNTs. Thus we believe that the EF will preferentially affect the growth of *m*-CNTs.

With respect to EF-assisted CVD growth of gas flow-directed ultralong CNTs, we suppose that the EF has no effect on *m*-CNTs and *s*-CNTs at the very beginning of CNT growth because the EF force on these CNTs is weaker [14,33]. During the lengthening of CNTs, say at the first stage of growth, the EF force will only operate on *m*-CNTs and cause them to align with the EF [14,15]. The perpendicular EF force can help with buoyancy, lifting more *m*-CNTs up into the laminar gas flow compared with an EF-free system (Fig. 4a and b), which promotes *m*-CNTs' growth. In other words, the EF helps *m*-CNTs grow more easily; therefore, more ultralong *m*-CNTs are obtained in CNT arrays far away from catalyst regions where

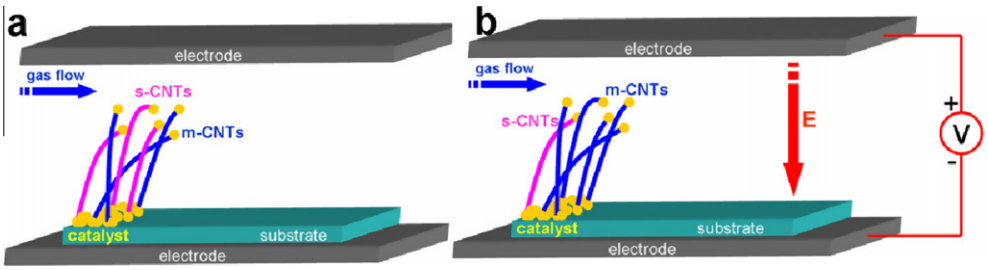

Fig. 4 – Illustration of the EF effect on the growth of *m*-CNTs and *s*-CNTs.

growth begins. For *s*-CNTs, the EF energy cannot overcome the thermal energy [14,33] and the EF force is negligible [14,15], so only buoyant forces can lift the tubes into the laminar gas flow at the vertical direction [29]. Due to the additional EF force on *m*-CNTs, EF-assisted CVD growth can increase the percentage of *m*-CNTs. We also carried out the Raman mapping characterization at the catalyst area to prove the above speculation, and the one result in Figure S5 in SI showed that *m*-CNTs and *s*-CNTs coexisted and their content is almost equal, which is an evidence that EF have no selectivity on the origin growth of *m*-CNTs and *s*-CNTs, but only take effect on the subsequent period of CNTs' growth.

It is remarkable that the EF force for *m*-CNTs is comparable to the gas flow orientation force, but they are oriented in different directions. The EF force along with the gas flow force will also disturb the *m*-CNTs' growth, making them vibrate. They are then likely to bump onto the substrate and stop growing. This is why fewer ultralong CNTs are observed at high EF intensities and the tortuous CNTs, illustrating the impact of the disturbance, are formed. As shown in Fig. 1b–f, the alignment of CNTs tends to be less regular when the EF is increased from 0 to 330 V/cm.

5. Summary

We reported an approach to increase the proportion of *m*-CNTs in ultralong aligned CNT arrays by EF-assisted CVD. It was found that the EF not only can affect the structure of ultralong CNT arrays but also can increase the percentage of *m*-CNTs due to the different polarizabilities of *m*-CNTs and *s*-CNTs. Electrical property measurements showed that more *m*-CNTs can be obtained under EF-assisted CVD because the EF force lifts more *m*-CNTs than *s*-CNTs into the laminar gas flow. The percentage of *m*-CNTs in ultralong CNT arrays can reach about 80% when EF intensity is 200 V/cm.

Acknowledgement

This work was supported by NSFC (50972001, 20725307, and 50821061) and MOST (2011CB932601).

Appendix A. Supplementary data

Supplementary data associated with this article can be found, in the online version, at doi:10.1016/j.carbon.2011.02.045.

REFERENCES

[1] Baughman RH, Zakhidov AA, de Heer WA. Carbon nanotubes – the route toward applications. Science 2002;297(5582):787–92.
[2] Chen ZH, Appenzeller J, Lin YM, Sippel-Oakley J, Rinzler AG, Tang JY, et al. An integrated logic circuit assembled on a single carbon nanotube. Science 2006;311(5768):1735.
[3] Javey A, Guo J, Wang Q, Lundstrom M, Dai HJ. Ballistic carbon nanotube field-effect transistors. Nature 2003;424(6949):654–7.
[4] Kong J, Franklin NR, Zhou CW, Chapline MG, Peng S, Cho KJ, et al. Nanotube molecular wires as chemical sensors. Science 2000;287(5453):622–5.
[5] Tans SJ, Devoret MH, Groeneveld RJA, Dekker C. Electron–electron correlations in carbon nanotubes. Nature 1998;394(6695):761–4.
[6] Bachtold A, Hadley P, Nakanishi T, Dekker C. Logic circuits with carbon canotube transistors. Science 2001;294(5545):1317–20.
[7] Krupke R, Hennrich F, von Lohneysen H, Kappes MM. Separation of metallic from semiconducting single-walled carbon nanotubes. Science 2003;301(5631):344–7.
[8] Arnold MS, Green AA, Hulvat JF, Stupp SI, Hersam MC. Sorting carbon nanotubes by electronic structure using density differentiation. Nat Nanotechnol 2006;1(1):60–5.
[9] Zhang GY, Qi PF, Wang XR, Lu YR, Li XL, Tu R, et al. Selective etching of metallic carbon nanotubes by gas-phase reaction. Science 2006;314(5801):974–7.
[10] Li YM, Mann D, Rolandi M, Kim W, Ural A, Hung S, et al. Preferential growth of semiconducting single-walled carbon nanotubes by a plasma enhanced CVD method. Nano Lett 2004;4(2):317–21.
[11] Ding L, Tselev A, Wang JY, Yuan DN, Chu HB, McNicholas TP, et al. Selective growth of well-aligned semiconducting single-walled carbon nanotubes. Nano Lett 2009;9(2):800–5.
[12] Hong G, Zhang B, Peng BH, Zhang J, Choi WM, Choi JY, et al. Direct growth of semiconducting single-walled carbon nanotube array. J Am Chem Soc 2009;131(41):14642–3.
[13] Harutyunyan AR, Chen GG, Paronyan TM, Pigos EM, Kuznetsov OA, Hewaparakrama K, et al. Preferential growth of single-walled carbon nanotubes with metallic conductivity. Science 2009;326(5949):116–20.
[14] Joselevich E, Lieber CM. Vectorial growth of metallic and semiconducting single-wall carbon nanotubes. Nano Lett 2002;2(10):1137–41.
[15] Zhang YG, Chang AL, Cao J, Wang Q, Kim W, Li YM, et al. Electric-field-directed growth of aligned single-walled carbon nanotubes. Appl Phys Lett 2001;79(19):3155–7.
[16] Ural A, Li YM, Dai HJ. Electric-field-aligned growth of single-walled carbon nanotubes on surfaces. Appl Phys Lett 2002;81(18):3464–6.

[17] Matsuda T, Mesko M, Ishikawa T, Sato J, Ogino A, Tamura R, et al. Role of negative electric field biasing on growth of vertically aligned carbon nanotubes using chemical vapor deposition. Japan J Appl Phys 2008;47(9):7436–9.
[18] Avigal Y, Kalish R. Growth of aligned carbon nanotubes by biasing during growth. Appl Phys Lett 2001;78(16):2291–3.
[19] Jiao LY, Fan B, Xian XJ, Wu ZY, Zhang J, Liu ZF. Creation of nanostructures with poly (methyl methacrylate)-mediated nanotransfer printing. J Am Chem Soc 2008;130(38):12612–3.
[20] Wang S, Liang XL, Chen Q, Yao K, Peng LM. High-field electrical transport and breakdown behavior of double-walled carbon nanotube field-effect transistors. Carbon 2007;45(4):760–5.
[21] Liu KH, Wang WL, Xu Z, Bai XD, Wang EG, Yao YG, et al. Chirality-dependent transport properties of double-walled nanotubes measured in situ on their field-effect transistors. J Am Chem Soc 2009;131(1):62–3.
[22] Radosavljevic M, Lefebvre J, Johnson AT. High-field electrical transport and breakdown in bundles of single-wall carbon nanotubes. Phys Rev B 2001;64(24):241307–10.
[23] Wang S, Liang XL, Chen Q, Zhang ZY, Peng LM. Field-effect characteristics and screening in double-walled carbon nanotube field-effect transistors. J Phys Chem B 2005;109(37):17361–5.
[24] Kozinsky B, Marzari N. Static dielectric properties of carbon nanotubes from first principles. Phys Rev Lett 2006;96(16):166801–4.
[25] Huang SM, Maynor B, Cai XY, Liu J. Ultralong, well-aligned single-walled carbon nanotube architectures on surfaces. Adv Mater 2003;15(19):1651–3.
[26] Huang SM, Cai XY, Liu J. Growth of millimeter-long and horizontally aligned single-walled carbon nanotubes on flat substrates. J Am Chem Soc 2003;125(19):5636–7.
[27] Huang SM, Cai XY, Du CS, Liu J. Oriented long single walled carbon nanotubes on substrates from floating catalysts. J Phys Chem B 2003;107(48):13251–4.
[28] Jin Z, Chu HB, Wang JY, Hong JX, Tan WC, Li Y. Ultralow feeding gas flow guiding growth of large-scale horizontally aligned single-walled carbon nanotube arrays. Nano Lett 2007;7(7):2073–9.
[29] Hofmann M, Nezich D, Reina A, Kong J. In-situ sample rotation as a tool to understand chemical vapor deposition growth of long aligned carbon nanotubes. Nano Lett 2008;8(12):4122–7.
[30] Incropera FP, DeWitt DP. Introduction to heat transfer. second ed. New York: John Wiley & Sons, Inc.; 1990.
[31] Fox RW, McDonald AT. Introduction to fluid mechanics. 5th ed. New York: John Wiley & Sons, Inc.; 1998.
[32] Benedict LX, Louie SG, Cohen ML. Static polarizabilities of single-wall carbon nanotubes. Phys Rev B 1995;52(11):8541–9.
[33] Hongo H, Nihey F, Ochiai Y. Horizontally directional single-wall carbon nanotubes grown by chemical vapor deposition with a local electric field. J Appl Phys 2007;101(2):024325–24333.